Non-cell autonomous control of apoptosis by ligand-independent Hedgehog signaling in *Drosophila*

AE Christiansen[1], T Ding[1], Y Fan[2], HK Graves[1], H-M Herz[3], JL Lindblad[2] and A Bergmann*,[2]

Hedgehog (Hh) signaling is important for development and homeostasis in vertebrates and invertebrates. Ligand-independent, deregulated Hh signaling caused by loss of negative regulators such as Patched causes excessive cell proliferation, leading to overgrowth in *Drosophila* and tumors in humans, including basal-cell carcinoma and medulloblastoma. We show that in *Drosophila* deregulated Hh signaling also promotes cell survival by increasing the resistance to apoptosis. Surprisingly, cells with deregulated Hh activity do not protect themselves from apoptosis; instead, they promote cell survival of neighboring wild-type cells. This non-cell autonomous effect is mediated by Hh-induced Notch signaling, which elevates the protein levels of *Drosophila* inhibitor of apoptosis protein-1 (Diap-1), conferring resistance to apoptosis. In summary, we demonstrate that deregulated Hh signaling not only promotes proliferation but also cell survival of neighboring cells. This non-cell autonomous control of apoptosis highlights an underappreciated function of deregulated Hh signaling, which may help to generate a supportive micro-environment for tumor development.

Cell Death and Differentiation (2013) **20**, 302–311; doi:10.1038/cdd.2012.126; published online 28 September 2012

Programmed cell death or apoptosis is a normal feature of organ development that counterbalances growth and allows shaping of the organ by eliminating cells.[1,2] Control of apoptosis comes down to the control of specific cell death proteases, termed caspases.[3] One class of caspase inhibitors are inhibitor of apoptosis proteins (IAPs). *Drosophila* IAP-1 (Diap-1) effectively inhibits the caspases Dronc (Caspase-9-like) and DrICE (Caspase-3-like).[1,2] The IAP antagonists Reaper, Hid and Grim stimulate ubiquitylation and degradation of Diap-1, releasing caspases from IAP inhibition.[4] This mechanism is tightly coordinated with mechanisms that regulate proliferation and growth to maintain tissue homeostasis.[5,6] However, although much is known about the individual processes of proliferation, growth and apoptosis, how these mechanisms tie together is not well understood.

The development of the *Drosophila* eye depends on a changing balance of proliferative growth, differentiation and apoptosis, providing an excellent system to study how these processes interact.[7,8] During the first two stages of larval development, the eye-antennal imaginal disc proliferates extensively, forming a bi-lobed structure. The antennal lobe will make the adult antenna, while the eye lobe will form the head capsule and eye. In the third larval stage, a wave of differentiation begins at the most posterior part of the eye lobe and is marked by the formation of a groove called the morphogenetic furrow (MF) that moves anterior. Cells at the MF arrest proliferation and begin to differentiate in a well-defined pattern with the formation of photoreceptor neuron clusters followed by support cells that will separate each cluster. Cells that remain unspecified undergo apoptosis during pupal development.[9]

In the MF, signaling pathways coordinate the transition from proliferation to differentiation. In a simplified summary, cells in the MF arrest in G1 in response to Decapentaplegic (Dpp), which is induced by Hedgehog (Hh) signaling.[10–13] Hh and Dpp also induce the expression of the Notch (N) ligand Delta, which, in turn, induces a round of mitosis (second mitotic wave) in cells just posterior to the MF.[11,14] Thus, the Hh pathway is needed for MF progression (Figure 1h) and coordinates the transition from proliferation to differentiation, making it a critical target for homeostasis.

Hh signal transduction is highly conserved between flies and mammals.[15,16] In cells that are not exposed to the Hh ligand, the transmembrane protein Patched (Ptc; Ptch1 in mammals) blocks the availability of another transmembrane protein, Smoothened (Smo).[17,18] In the absence of Smo, Costal-2 (Cos2), which encodes a kinesin-like protein with similarity to mammalian Kif-7 (kinesin family member 7),
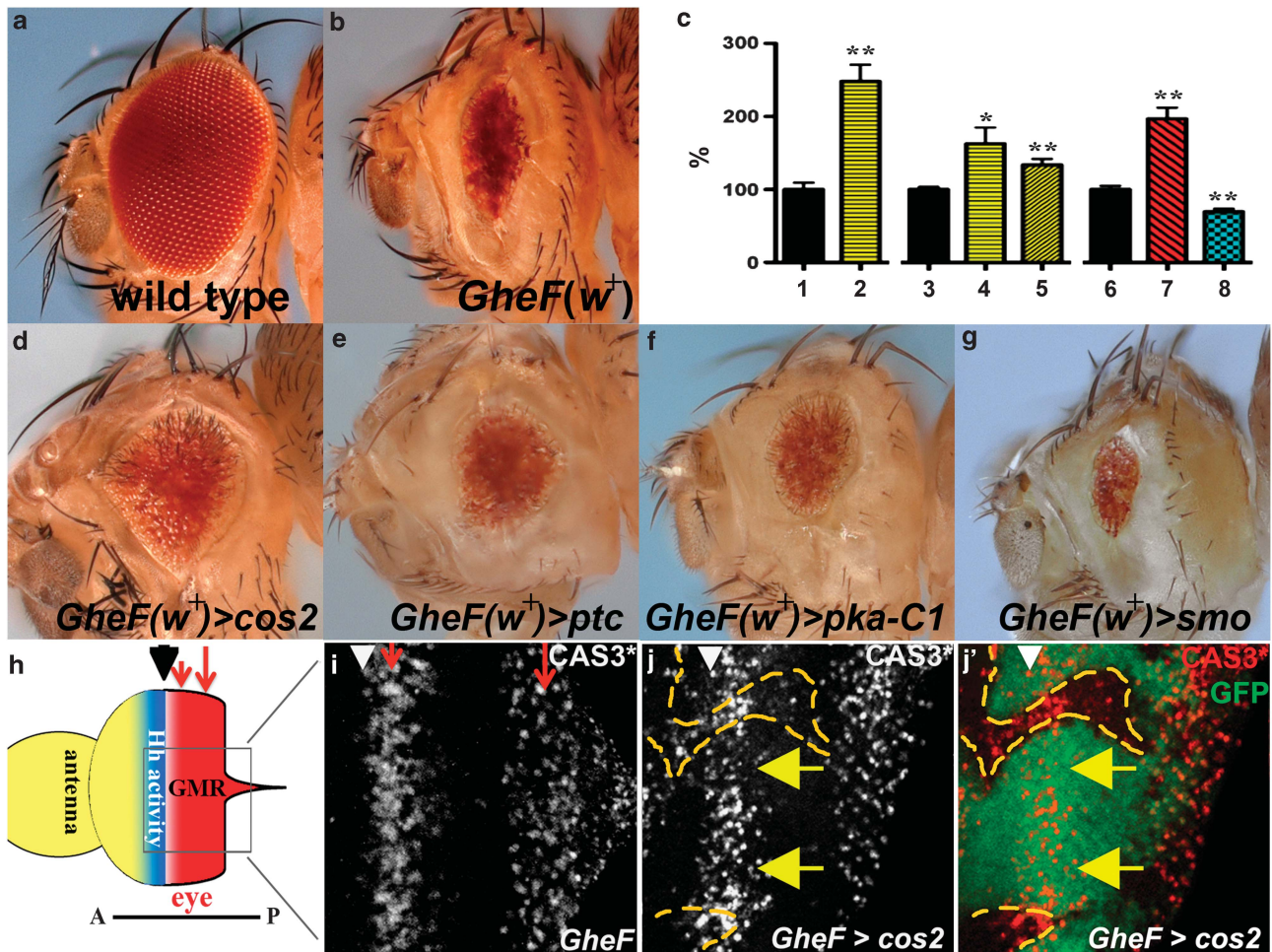
Figure 1 Mutants of negative regulators of Hh signaling suppress *GMR-hid* by non-cell autonomous inhibition of caspase activity. In this and the following figures, > denotes an FRT site, indicating mitotic or *FLP*-out clones. Adult eye images are of *GMR-hid* females unless otherwise specified. Anterior is to the left. The location of the MF is marked by arrowheads. (**a**) Wild-type eye. (**b**) The *GMR-hid ey-FLP* (*GheF*) eye ablation phenotype. Note, this transgene carries the P[w^+] marker gene. (**c**) Histogram of relative eye size of different genotypes. Eyes from *GMR-hid* flies (black bars) are normalized to 100%; 1 and 2 are male flies, 3–8 are females. *cos2* (yellow bars) and *pka-C1* (red bar) mosaics increase the average *GMR-hid* eye size, whereas *smo* mosaics (blue bar) decreases the average eye size. For each bar, 10 eyes were averaged, except 8 (5 eyes). *P-value ≤0.05 and **P-value ≤0.01. 1, *GMR-hid ey-FLP/Y*; *FRT42D P[ubi-GFP]/CyO* male. 2, *GMR-hid ey-FLP/Y*; *FRT42D cos2^{H29}/FRT42D P[ubi-GFP]* male. 3, *GMR-hid ey-FLP/y w*; *FRT42D P[ubi-GFP]/CyO* female. 4, *GMR-hid ey-FLP/y w*; *FRT42D cos2^{H29}/FRT42D P[ubi-GFP]* female. 5, *GMR-hid ey-FLP/y w*; *FRT42D cos2^{L51}/ FRT42D P[ubi-GFP]* female. 6, *ey-FLP/y w*; P(w^+) *FRT40A/ CyO*; *GMR-hid/+* female. 7, *ey-FLP/y w*; *pka-c1^{K2} FRT40A/ P(w^+) FRT40*; *GMR-hid/+* female. 8, *ey-FLP/y w*; *smo^{D16} FRT40A/ P(w^+) FRT40*; *GMR-hid/+* female. (**d–f**) The *GheF* phenotype is suppressed (eyes are larger) when flies are mosaic for either *cos2* (**d**), *ptc* (**e**), or *pka-C1* (**f**) mutations (quantified in (**c**)). (**g**) The *GheF* phenotype is enhanced when flies are mosaic for *smo*, a positive regulator of Hh signaling. (**h**) Schematic outline of an eye-antennal imaginal disc from a third instar larvae. The MF (arrowhead) separates anterior (A) and posterior (P) portions of the eye disc. Hh activity (blue) is required for anterior progression of the MF. *GMR* is expressed posterior to the MF (red). *GMR-hid* induces two apoptotic waves (red arrows). (**i**) In *GMR-hid* eye discs, cleaved Caspase-3 (CAS3*) antibody as apoptosis marker labels two distinct waves (red arrows) posterior to the MF.[30] (**j** and **j′**), A *GMR-hid* eye disc mosaic for *cos2*. *cos2* clones are marked by the absence of GFP and outlined by yellow dashed lines. CAS3* labeling is high in *cos2* clones but low in adjacent non-mutant tissue near the MF (yellow arrows). Genotypes: (**b**) *y w GMR-hid ey-FLP*; *FRT42D P[ubi-GFP]/CyO*. (**d** and **e**) *y w GMR-hid ey-FLP*; *FRT42D cos2^{H29}* (**d**) or *ptc^C* (**e**)/*FRT42D P[w$^+$]*. (**f** and **g**) *y w GMR-hid ey-FLP*; *pka-c1^{B3}* (**f**) or *smo^{D16}* (**g**) *FRT40A/P[w$^+$] FRT40*. (**i**) *y w GMR-hid ey-FLP*; *FRT42D P[ubi-GFP]/CyO*. (**j** and **j′**) *y w GMR-hid ey-FLP*; *FRT42 cos2^{H29}/FRT42 P[ubi-GFP]*

associates in a complex with the transcription factor Cubitus interruptus (Ci) that promotes proteolytic processing of Ci to the truncated repressor, CiR.[19–24] When Hh binds Ptc, Smo becomes available, interacts with Cos2 and triggers release of full-length Ci, which can then function as a transcriptional activator (CiA).

Genetically, *ptc* and *cos2* (and another component, protein kinase A (*PKA*)) are negative regulators of Hh signaling promoting the formation of CiR.[15,16] Thus, genetic inactivation

of *ptc*, *cos2* and *pka* triggers ligand-independent, deregulated Hh signaling due to accumulation of CiA. In humans, ligand-independent Hh signaling is associated with several tumors such as basal cell carcinoma, medulloblastoma, rhabdomyosarcoma and glioma.[25] In most cases, either genetic inactivation of *Ptch1* or activating missense mutations of *smo* are the underlying causes of these tumors.

Apoptosis can be induced in the larval eye disc to determine how the tissue responds when the balance between

proliferation, differentiation and cell death is tilted by increased apoptosis. Using this system, we have identified several pathways that function in regulating tissue homeostasis.[26–29] Here, we show that in genetic mosaics, ligand-independent, deregulated Hh signaling due to loss of negative regulators suppresses excessive cell death. Interestingly, this control of apoptosis affects cells of the two genotypes differently. It is not the cells with increased Hh signaling that are resistant to apoptosis. Instead, these cells instruct neighboring wild-type cells to increase their apoptosis resistance. This non-cell autonomous effect is mediated through Hh-induced stimulation of the N pathway, which then transcriptionally increases the levels of Diap-1 in neighboring cells. This non-cell autonomous control of apoptosis highlights an underappreciated function of Hh signaling. The increased resistance to apoptosis in cells adjacent to cells with deregulated Hh signaling may change the micro-environment, providing an additional role for deregulated Hh signaling needed for efficient tumorigenesis in human cancer.

Results

Mutants of negative regulators of Hh signaling suppress apoptosis by non-cell autonomous inhibition of caspase activity.

Expression of the pro-apoptotic gene *hid* posterior to the MF using the *GMR* promoter (*GMR-hid*) induces an eye-ablation phenotype due to massive apoptosis[30] (Figures 1b, h and i). We are using the *GMR-hid* system to identify suppressor mutations that confer resistance to apoptosis. To identify suppressors, we performed a mutagenesis screen in a *GMR-hid* background by generating genetic mosaics using the *ey-FLP/FRT* system (*GheF* screen), as described.[31,32] Negative regulators of Hh signaling, including *cos2*, *ptc* and the catalytic subunit of PKA, *pka-C1*, were identified as moderate suppressors of *GMR-hid* (Figures 1d–f; quantified in Figure 1c; see Material and Methods section). Heterozygosity of these mutants does not dominantly suppress *GMR-hid* (see Supplementary Figure S1), indicating that they are recessive suppressors. By contrast, mosaic loss of the positive regulator *smo* enhances the *GMR-hid* eye phenotype (Figure 1g). Therefore, ligand-independent, deregulated Hh signaling by loss of negative regulators suppresses *GMR-hid*-induced apoptosis, whereas loss of positive regulators enhances it.

Components of the Hh pathway are known to regulate eye growth[14,33–35] but have not been described as regulating apoptosis previously. To further characterize the suppression of *GMR-hid*, we examined *cos2* mosaic *GMR-hid* eye imaginal discs with cleaved Caspase-3 (CAS3*) antibody as apoptosis marker.[30] *GMR-hid* induces two waves of apoptotic cells posterior to the MF (Figures 1h and i, red arrows).[30] Surprisingly, in *cos2* mosaic *GMR-hid* eye discs, CAS3* labeling is not reduced in *cos2* clones overlapping with the apoptotic waves (Figures 1j and j′). By contrast, wild-type or heterozygous (referred to as non-mutant) cells immediately adjacent to *cos2* clones show decreased CAS3* labeling (yellow arrows in Figures 1j and j′; see Supplementary Figure S2). Therefore, while *cos2* clones themselves are unprotected from *GMR-hid*-induced apoptosis, they appear to

increase the apoptosis resistance of neighboring non-mutant cells. The non-cell autonomous suppression of *GMR-hid* by *cos2* clones occurs only in the first apoptotic wave located at the MF (Figures 1h i, j, and j″; see Supplementary Figure S2). *cos2* clones do not affect the second apoptotic wave, explaining the moderate suppression of *GMR-hid* by *cos2* (Figure 1d). Thus, mutants of negative regulators of the Hh pathway, which cause ligand-independent Hh activity, suppress *GMR-hid* through non-cell autonomous inhibition of caspase activity.

Non-cell autonomous suppression of *GMR-hid* by ligand-independent Hh signaling.

Because of the surprising observation that *cos2* clones promote non-cell autonomous suppression of *GMR-hid*-induced apoptosis, we sought an unambiguous assay to identify the genetic identity of the rescued eye tissue in *cos2*, *ptc* and *pka-C1* mosaic *GMR-hid* flies. The original *GMR-hid* transgene is marked with the white[+] (w^+) pigment marker, producing red eye pigment in mutant and wild-type cells (Figure 1b) and precluding an analysis of cell autonomy by eye pigmentation. Instead, we used a *GMR-hid* transgene without the w^+ pigment gene causing a white eye of reduced size (referred to as *GheF(w⁻)*), Figure 2a). A w^+ marker on the homologous chromosome arm allows determination of the genetic identity of the surviving tissue in genetic eye mosaics (Figure 2b). If the surviving tissue is white (w^-) and thus mutant, the suppression is autonomous: a mosaic of *Uba1*, a known autonomous suppressor of *GMR-hid*,[27] is shown in Figure 2f. However, if the surviving tissue is red (w^+) and thus non-mutant, then the suppression is non-cell autonomous (Figure 2b). Mosaic *cos2*, *ptc* and *pka-C1* eyes in a *GheF(w⁻)* background are composed of almost entirely red (w^+) non-mutant tissue (Figures 2c–e), indicating non-cell autonomous suppression of *GMR-hid*, consistent with the CAS3* analysis in Figure 1j.

This result is remarkable. Normally, wild-type and heterozygous *cos2*, *ptc* and *pka-C1* cells are susceptible to *GMR-hid*-induced apoptosis (see Supplementary Figure S1). However, while *cos2*, *ptc* and *pka-C1* mutant clones are unprotected from *GMR-hid*-induced apoptosis and do not contribute to the rescued eye tissue, they appear to increase the apoptosis resistance of neighboring non-mutant tissue, leading to suppression of the strong apoptotic phenotype of *GMR-hid*. These observations imply that cells with deregulated Hh activity produce a signal that increases the apoptosis resistance of neighboring cells.

Hh activity is mediated by the transcription factor Ci.[15,16] In the absence of Hh, Ci is proteolytically processed to the repressor form CiR.[15,36] Hh signaling or loss of negative Hh pathway regulators maintain full-length Ci (CiA).[15] To test whether activation of Ci accounts for the suppression of *GMR-hid* (Figures 2g and i), we blocked Ci activity in *cos2* clones by overexpression of CiR. Consistently, expression of *CiR* in *cos2* clones reverts the suppression of *GMR-hid* by *cos2* (Figure 2j) and restores the normal CAS3* pattern (Supplementary Figure S3). Expression of *CiR* alone does not grossly modify *GMR-hid* (Figure 2h). These data suggest that the non-cell autonomous resistance to apoptosis in *cos2* mosaics is mediated by inappropriate Ci activation.
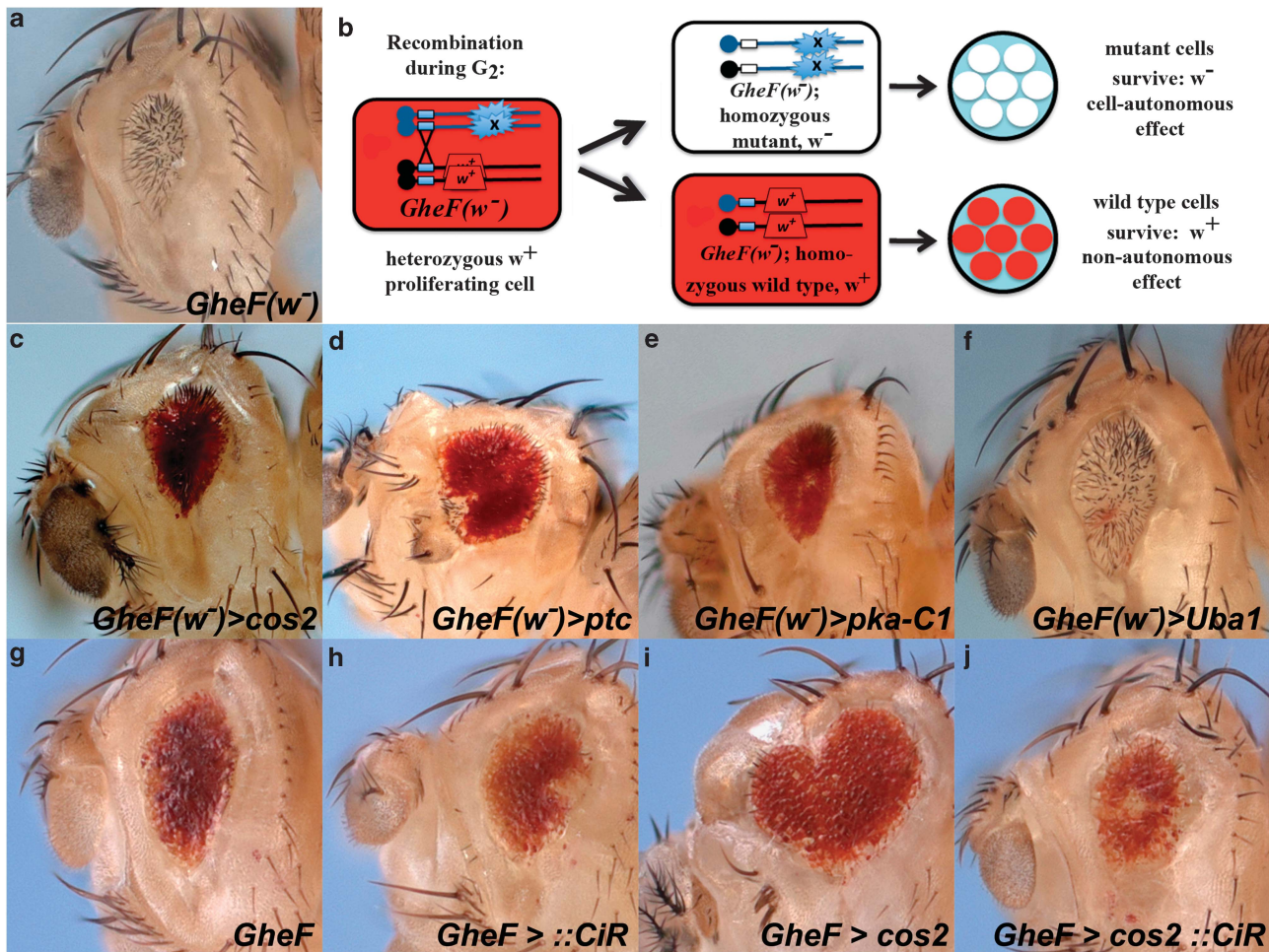
Figure 2 Negative regulators of Hh signaling are non-cell autonomous suppressors of *GMR-hid*. In this and the following figures, :: denotes expression from a *UAS*-based transgene. (**a**) The *GMR-hid(w⁻) ey-FLP* (*GheF(w⁻)*) eye ablation phenotype. (**b**) Schematic for determination of the autonomy/non-autonomy of surviving tissue in mutant mosaics in *GheF(w⁻)* background. (**c–e**) The suppressed *GheF(w⁻)* eye by *cos2* (**c**), *ptc* (**d**) or *pka-C1* (**e**) mosaics is nearly all red (*w⁺*), thus comprised of non-mutant tissue and indicating non-cell autonomous suppression. (**f**) *Uba1*, a known autonomous suppressor,[27] serves as a positive control for autonomous suppression of *GheF(w⁻)* as revealed by a white (*w⁻*) suppressed eye. (**g–j**) Ectopic expression of *CiR* using the MARCM system (Material and Methods section) abrogates *cos2* suppression of *GMR-hid*. Suppression of *GMR-hid* by *cos2* mosaics (**i**) is reversed by co-expression of *CiR* (**j**). Expression of *CiR* alone (**h**) has no effects on *GMR-hid* (**g**). Genotypes: (**c** and **d**) *y w ey-FLP*; *FRT42D cos2^H29*(**c**) or *ptc^C*(**d**)/*FRT42D P[w⁺]*; *GMR-hid(w⁻)*. (**e**) *y w ey-FLP*; *pka-c1^K2 FRT40/P[w⁺] FRT40*; *GMR-hid(w⁻)*. (**f**) *y w ey-FLP*; *FRT42D Uba1^H42/FRT42D P[w⁺]*; *GMR-hid(w⁻)*. (**g**) *y w GMR-hid ey-FLP*; *FRT42 tubP-GAL80/CyO*; *tubP-GAL4/UAS-Ci^CE*. (**h**) *y w GMR-hid ey-FLP*; *FRT42 tubP-GAL80/FRT42*; *tubP-GAL4/UAS-Ci^CE*. (**i**) *y w GMR-hid ey-FLP*; *FRT42 cos2^H29/FRT42 tubP-Gal80*; *tubP-GAL4/TM6B*. (**j**) *y w GMR-hid ey-FLP*; *FRT42 cos2^H29/FRT42 tubP-Gal80*; *tubP-GAL4/UAS-Ci^CE*

Non-cell autonomous upregulation of Diap1 by ligand-independent Hh signaling. To determine the mechanism of increased non-cell autonomous resistance to apoptosis, we examined the protein levels of Diap-1, an inhibitor of apoptosis,[37–41] in *cos2* mosaic eye discs (without *GMR-hid*). Diap-1 is the rate-limiting component in the apoptosis pathway, and Diap-1 protein levels determine the apoptosis threshold. Significantly, Diap-1 protein accumulates just outside of *cos2* clones (Figures 3a, a′ and a″, arrows), consistent with the non-cell autonomous suppression of apoptosis. Furthermore, heterozygosity of *diap-1* reverts the suppression of *GMR-hid* in *cos2* mosaics (see Supplementary Figure S4), suggesting that Diap-1 is genetically required for suppression of *GMR-hid* in *cos2* mosaics. We did not detect any significant changes in the protein levels of other cell death pathway components,

including the caspases Dronc and DrICE. Therefore, cells with deregulated Hh signaling promote upregulation of Diap-1 in neighboring cells, which increases their apoptosis resistance and protects them from *GMR-hid*-induced apoptosis. The non-cell autonomous upregulation of Diap-1 is best detectable in or anterior to the MF (Figures 3a, a′ and a″). It is difficult to judge whether *cos2* clones posterior to the MF also increase Diap-1 levels non-cell autonomously because endogenous Diap-1 levels are high (Figures 3a, a′ and a″). However, as shown below, Hh activity is also increased immediately posterior to the MF.

To address whether Ci mediates the non-cell autonomous increase of Diap-1, we examined Diap-1 levels in mosaic discs of regulators of Ci processing. Anterior to the MF, processing of CiA to CiR requires a Cullin-1 (Cul-1) and Nedd8-dependent ubiquitylation event, mediated by the
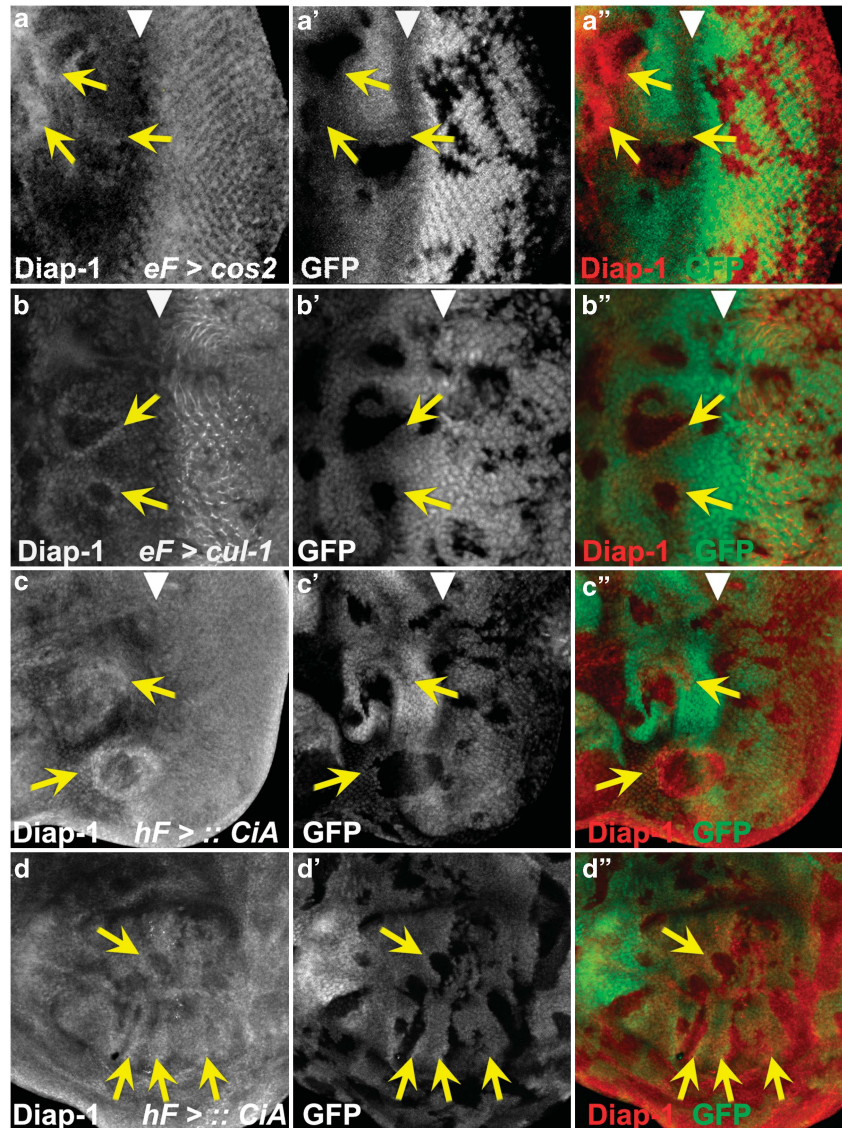
Figure 3 CiA-dependent non-cell autonomous accumulation of Diap-1 anterior to the MF. (**a**, **a′** and **a″**) *cos2* and (**b**, **b′** and **b″**) *cul-1* mosaic eye discs were labeled with anti-Diap-1 antibody. Mutant clones are marked by the absence of GFP. Clones located in or anterior to the MF (arrowhead) promote non-cell autonomous increase of Diap-1 levels (arrows). In contrast to *cos2*, mutant clones of *cul-1* posterior to the MF contain reduced levels of Diap-1, indicating a requirement of *cul-1* for Diap-1 regulation in addition to its role in Hh signaling. *eF* = *ey-FLP*. (**c** and **d**) Ectopic expression of *CiA* induces non-cell autonomous increase of Diap-1 levels in (**c**, **c′** and **c″**) eye and (**d**, **d′** and **d″**) wing discs (arrows). *CiA*-expressing clones are marked by the absence of GFP. *hF* = *hs-FLP*. Panels (**a**–**d**) show the Diap-1 labelings only; panels (**a′**–**d′**) show the GFP channel only; panels (**a″**–**d″**) show the merge of Diap-1 and GFP. Genotypes: (**a** and **b**) *y w ey-FLP*; *FRT42D cos2^H29*(**a**) or *cul-1^EX* (**b**)/*FRT42D P[ubi-GFP]*. (**c** and **d**) *y w hs-FLP*; *P[tubP > GFP > GAL4]*; *UAS-CiA*. (> denotes *FRT*)

ubiquitin ligase Slimb (Slmb).[36,42–44] Loss of these genes causes accumulation of active CiA,[36] similar to *cos2* mutants. Consistently, non-mutant cells immediately adjacent to *cul-1*, *nedd8* and *slmb* clones have increased levels of Diap-1 in or anterior to the MF similar to *cos2* (Figures 3b and b′ and see Supplementary Figures S4d and e), suggesting that lack of CiA processing promotes non-cell autonomous increase of Diap-1. Furthermore, clonal overexpression of *CiA* induces a non-cell autonomous increase of Diap-1 in eye discs (Figure 3c). This effect is best visible in or anterior to the MF, but can also be detected immediately posterior to the MF (Figure 3c). In addition, *CiA*-expressing clones in wing imaginal discs also increased Diap-1 levels non-cell autonomously in a position-dependent manner in the wing pouch (Figure 3d).

The non-cell autonomous accumulation of Diap-1 occurs transcriptionally, as indicated by the non-cell autonomous induction of the transcriptional reporter *diap1-lacZ* in *cos2* and *ptc* mosaics (Figures 4a and b). The upregulation of the *diap1-lacZ* reporter is best detectable in or anterior to the MF, but some clones also show an effect immediately posterior to the MF (white arrow in Figure 4a′). To further clarify the position-dependence in *cos2* mosaics, we used a different marker of Hh signaling. Ptc is a transcriptional target of CiA[45] and can be
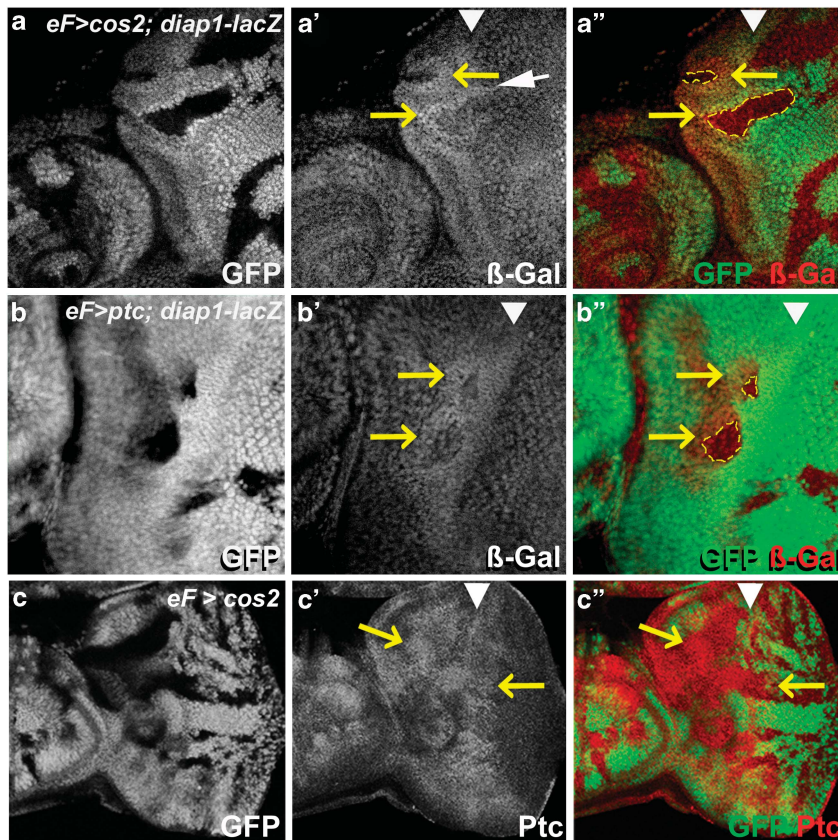
Figure 4 Non-cell autonomous upregulation of *diap1* transcription by deregulated Hh signaling. (**a** and **b**) An enhancer trap insertion in the *diap1* locus, *diap1-lacZ* (*th^{j5c8}*), was used as a reporter for *diap1* transcription. In both *cos2* (**a**) and *ptc* (**b**) mosaics, ß-GAL levels are increased (yellow arrows in **a′**, **a″**, **b′** and **b″**) anterior to the MF (white arrowheads) outside of the mutant clones (yellow outline in **a″** and **b″**). However, there is also non-cell autonomous induction of *diap1-lacZ* immediately posterior to the MF (white arrow in **a′**). (**c**, **c′**, **c″**) A *cos2* mosaic eye disc labeled with anti-Ptc antibody. Genotypes: (**a**) *ey-FLP*; *FRT42 cos2^{H29}/FRT42 P[ubi-GFP]*; *th^{j5c8}/+* . (**b**) *ey-FLP*; *FRT42 ptc^{X115}/FRT42 P[ubi-GFP]*; *th^{j5c8}/+* . (**c**) *ey-FLP*; *FRT42 cos2^{H29}/FRT42 P[ubi-GFP]*

used as a Hh marker. Consistent with the Diap1 and *diap1-lacZ* labelings, Ptc protein is upregulated in *cos2* mutant clones anterior to the MF and in the antennal dics (Figure 4c). Interestingly, while *cos2* clones located in the far posterior section of the eye disc do not change Ptc protein levels, *cos2* clones located immediately posterior to the MF also accumulate Ptc protein (Figure 4c). Therefore, while clones with deregulated Hh activity show the strongest phenotypes anterior to the MF, they also affect the area immediately posterior to the MF. This area overlaps with the first apoptotic wave (Figure 1i) explaining why only the first apoptotic wave of *GMR-hid* is suppressed in *cos2* mosaics (Figure 1j; Supplementary Figure S2).

We considered several signaling pathways that are activated in signal-receiving cells by deregulated Hh signaling in *cos2* clones, including the Hippo/Warts/Yorkie pathway, a growth control pathway known to control *diap1* transcription.[46] To monitor Hippo/Warts/Yorkie signaling, we used an enhancer trap insertion in the expanded (*ex*) gene (*ex-lacZ*), a target of Hippo/Warts/Yorkie signaling. However, *ex-lacZ* labeling is not significantly induced in *cos2* and *ptc* mosaic eye imaginal discs (Supplementary Figure S5), excluding the Hippo/Warts/Yorkie pathway as the target of deregulated Hh signaling in eye discs.

Notch is required for *cos2* suppression of *GMR-hid* and promotes Diap-1 accumulation non-cell autonomously. Hh activity produces several signaling molecules in the MF that activate Dpp, EGFR and N pathways for regulation of proliferation and differentiation in the eye disc.[8,11,13] Although we cannot exclude a role of EGFR and Dpp signaling, five lines of evidence implicate the N pathway for control of non-cell autonomous survival. First, the suppression of *GMR-hid* in *cos2* mosaics is abrogated by reduced N pathway activity (e.g., heterozygosity for *N* or the ligands *Dl* and *Serrate* (*Ser*)) (Figures 5a–d). Furthermore, heterozygosity of *Dl* and *Ser* suppresses the non-autonomous accumulation of Diap1 in *cos2* mosaics (Supplementary Figure S6). Therefore, the suppression of *GMR-hid* and non-autonomous accumulation of Diap1 in *cos2* mosaics depends on N activity. Second, protein levels of Dl are increased in *cos2* mutant clones (see Supplementary Figure S7a). The accumulation of Dl is dependent on Ci activity, because overexpression of CiR in *cos2* clones suppresses the upregulation of Dl (Supplementary Figure S7b). Surprisingly, protein levels of N itself also accumulate in *cos2* clones in and anterior to the MF (Figures 5e and e′). It is unknown how N levels accumulate in cells with deregulated Hh activity, but it suggests that Hh not only controls Dl but also N.
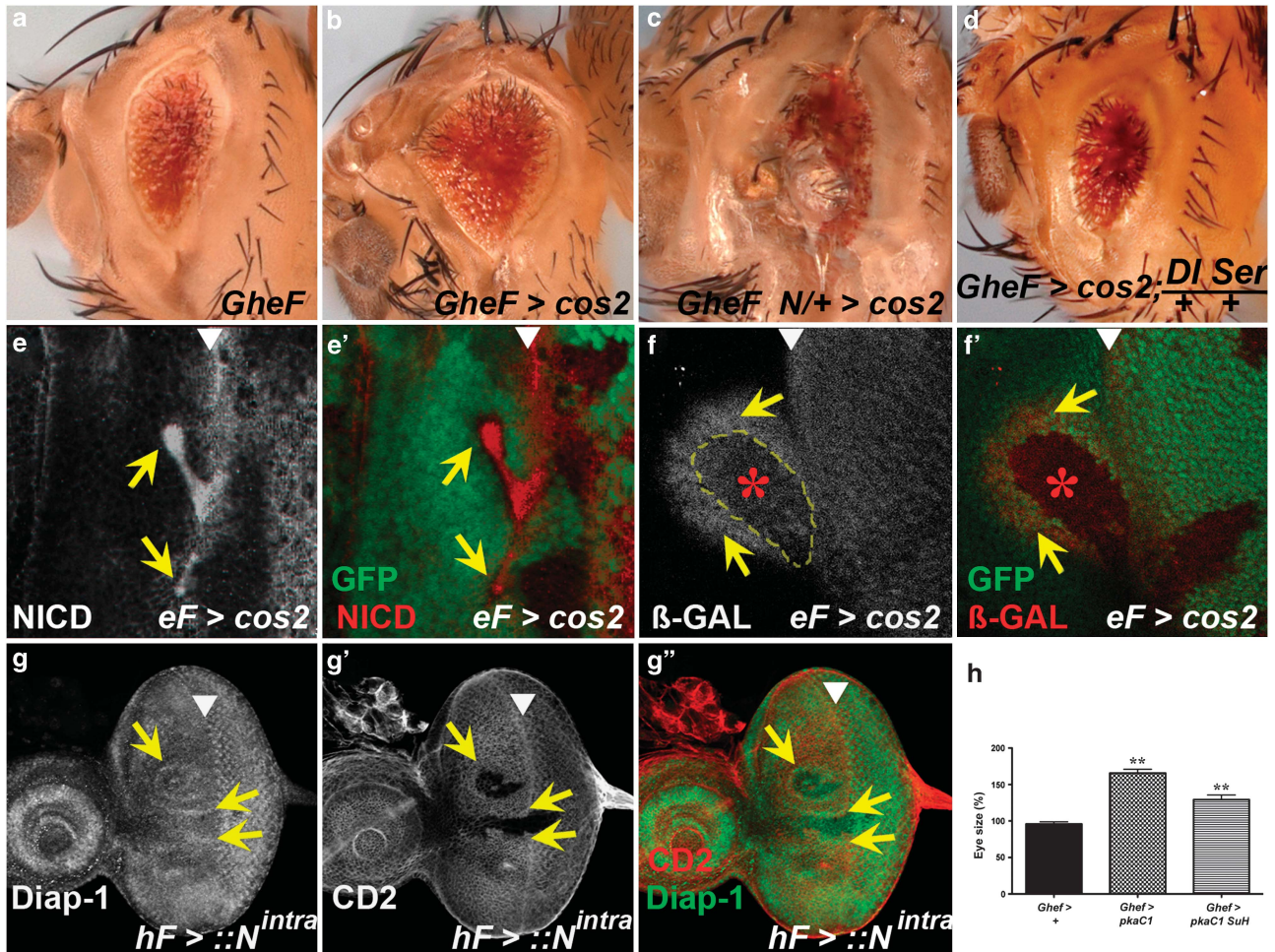
Figure 5 *Notch* is required for *cos2* suppression of *GMR-hid* and promotes Diap-1 accumulation non-cell autonomously. (**a–d**) Heterozygosity of *N* (**c**) or *Dl Ser* (**d**) reverts the suppression of *GMR-hid* in *cos2* mosaics (**b**), suggesting that Notch signaling is required for suppression of *GMR-hid* in *cos2* mosaics. (**e** and **e′**) N protein strongly accumulates in *cos2* clones (arrows) in or anterior to the MF (arrowhead). The N antibody (clone No. C17-9C6) was raised against the intracellular domain of N (NICD). (**f** and **f′**) *cos2* induces N activity autonomously (red star) and non-cell autonomously (yellow arrows) anterior to the MF (arrowhead) as shown by an *E(spl)m8-2.61-lacZ* reporter expressing ß-GAL. (**g**, **g′** and **g″**) Ectopic expression of the active form of N, N^{intra}, induces Diap-1 levels non-cell autonomously immediately adjacent to N^{intra}-expressing clones (arrows), located in or anterior to the MF (arrowhead). N^{intra}-expressing clones are marked by the absence of the CD2 marker. (**h**) Statistical analysis of the suppression of *GMR-hid* by *pka-C1* mosaics and *pka-C1 Su(H)* double mosaics. Eyes from *GMR-hid* flies are normalized to 100%. The suppression is partially reversed in double mosaics. For each bar, 10 eyes were averaged. **P-value ≤ 0.01. Genotypes: (**a**) *y w GMR-hid ey-FLP/+ ; FRT42D P[w+]/CyO*. (**b**) *y w GMR-hid ey-FLP/+ ; FRT42D cos2^{H29}/FRT42D P[w+]*. (**c**) *y w GMR-hid ey-FLP/N^8; FRT42D cos2^{H29}/FRT42D P[w+]*. (**d**) *y w GMR-hid ey-FLP/+ ; FRT42D cos2^{H29}/FRT42D P[w+]; Dl^{RevF10} Ser^{RX82}/+ .* (**e** and **e′**) *y w ey-FLP; FRT42D cos2^{H29}/FRT42D P[ubi-GFP]*. (**f** and **f′**) *y w ey-FLP; FRT42D cos2^{H29}P[E(spl)m8-2.61-lacZ]/FRT42D P[ubi-GFP] P[E(spl)m8-2.61-lacZ]*. (**g**, **g′** and **g″**) *y w hs-FLP/+ ; P[Act5c>CD2>GAL4]; UAS-N^{intra}/+ .* (**h**) *GMR-hid ey-FLP/+ ; P[ubi-GFP] FRT40/FRT40; GMR-hid ey-FLP/+ ; P[ubi-GFP] FRT40/pka-C1^{B3} FRT40; GMR-hid ey-FLP/+ ; P[ubi-GFP] FRT40/pka-C1^{B3} Su(H)$^{\Delta147}$ FRT40*

Third, *cos2* clones induce N activity autonomously and non-cell autonomously. Eye discs with *cos2* clones in or anterior to the MF show an autonomous increase of the N activity marker *E(spl)m8-2.61-lacZ* (Figures 5f and f′, red star). Importantly, there is also a strong non-cell autonomous increase of *E(spl)m8-2.61-lacZ* expression in non-mutant cells adjacent to anteriorly localized clones (Figures 5f and f′, yellow arrows), indicating increased non-cell autonomous N activity. We characterized the autonomous and non-cell autonomous N activity further. Both components of N activity are dependent on Ci signaling, because overexpression of CiR in *cos2* clones blocks *E(spl)m8-2.61-lacZ* expression anterior to the MF (Supplementary Figure S7c). As expected, the non-cell

autonomous component of N activity is dependent on Dl (Supplementary Figure S7d and e), consistent with the observations that removing Dl reverts the suppression of *GMR-hid* (Figure 5d) and suppresses the non-autonomous accumulation of Diap1 in *cos2* mosaics (Supplementary Figure S6). Fourth, clones of a different mutant, *vps25*, which is characterized by strong N activity, cause non-autonomous accumulation of Diap-1 protein.[26]

Fifth, clones of cells expressing the active form of N (N^{intra}) cause non-cell autonomous accumulation of Diap-1 in neighboring cells (Figures 5g, g′ and g″). This observation demonstrates that N does not directly induce *diap1* transcription, but generates another signal that promotes *diap1*

expression in neighboring cells (see Discussion section). Therefore, N relays the signal from cells with deregulated Hh signaling for Diap-1 induction in neighboring cells.

Because of the induction of both autonomous and non-cell autonomous N signaling in clones with deregulated Hh signaling, we also examined whether both the components of N signaling contribute to the suppression of *GMR-hid* by deregulated Hh signaling. For that purpose, we blocked autonomous N activity in *pka-C1* mutant clones by removing *Su(H)* function, which is required for transcriptional activity of N.[47] Interestingly, the suppression of *GMR-hid* by *pka-C1* mosaics is partially reverted by loss of *Su(H)* function and thus loss of autonomous N signaling (Figure 5h). These observations suggest that both autonomous and non-cell autonomous N activation contribute to the suppression of *GMR-hid*.

Discussion

We showed that deregulated Hh signaling in the eye disc through loss of the negative regulators *cos2*, *ptc* or *pka* triggers both autonomous and non-cell autonomous N activation in a CiA-dependent manner (see model in Figure 6). Although it is unknown how deregulated Hh signaling promotes autonomous N activity, the non-cell autonomous component of N signaling is mediated by Hh-dependent Dl expression (Supplementary Figure S7a).[11,14] Once N has been activated, it promotes non-cell autonomous expression of *diap1* in neighboring cells (Figure 5g). Therefore, at a clonal boundary of deregulated Hh signaling, there are two parallel events leading to N-dependent induction of *diap1* transcription in neighboring wild-type cells (Figure 6). In the first event, autonomous N signaling in *cos2* mutant cells directly generates an extracellular signal that induces *diap1* transcription in neighboring non-mutant cells (illustrated in purple in Figure 6). The molecular identity of this signal is unknown. In the second event, Dl triggers the non-cell autonomous component of N activation in neighboring non-mutant cells (illustrated in green in Figure 6). Non-cell autonomous N likely produces the same extracellular signal as autonomous N and triggers upregulation of *diap1* one cell further, thus acting as a relay of the Hh-derived signal for Diap-1 upregulation in neighboring cells. In this manner, upregulation of Diap-1 occurs in a stripe of at least two cells wide surrounding clones of deregulated Hh signaling. Depending on the range of the signal released by N, Diap-1 upregulation may extend even further. In addition, we observe non-cell autonomous N activity further away from the clone than one cell diameter (Figure 5f). This expansion may be due to cytoplasmic extensions such as cytonemes or additional relay mechanisms, and may increase Diap-1 levels further away from the clone. Therefore, when the MF in *GMR-hid* discs approaches a clone of deregulated Hh activity, it encounters higher levels of Diap-1, which protect neighboring cells from *hid*-induced apoptosis and causes the suppression of the *GMR-hid* eye phenotype.

The identity of the extracellular signal generated by N that triggers expression of *diap1* in neighboring wild-type cells is unknown. We tested the Hippo/Warts/Yorkie growth control pathway, which is known to regulate *diap1* transcription. However, our data did not support an involvement of
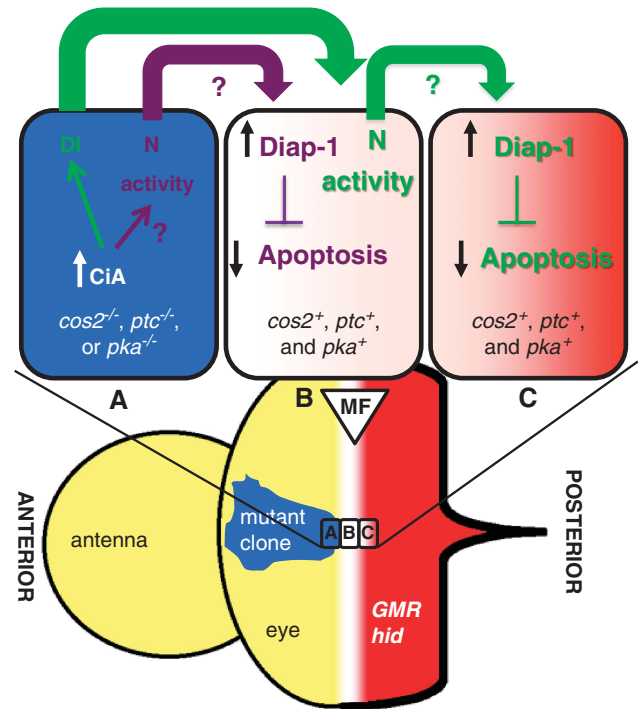

Figure 6 Model of non-cell autonomous induction of Diap-1 by cells with ligand-independent deregulated Hh activity. Drawn are three cells at a clonal boundary in the MF, one mutant cell (cell A) with deregulated Hh activity (blue) and two non-mutant cells (cells B and C; white to light red). The mutant cell accumulates CiA, which promotes autonomous N activity (purple arrow) and stimulates Dl expression (green arrow). Autonomous N signaling releases an unknown extracellular factor that promotes transcription of *diap1* in the first signal-receiving non-mutant cell, cell B. In the same non-mutant cell, Dl induces non-cell autonomous N activity, which in turn promotes transcription of *diap1* in the second non-mutant cell, cell C. In this manner, cells with deregulated Hh signaling transmit increased apoptosis resistance to neighboring cells by upregulation of Diap-1. When the MF moves into clones of deregulated Hh activity, *GMR*-driven *hid* expression (red) will be inhibited by increased Diap-1 levels, resulting in suppression of the *GMR-hid* eye phenotype. The white-to-red color gradient in cells B and C indicates the approaching *hid*-expressing wave driven by *GMR*

this pathway for non-autonomous induction of *diap1* in mosaic *cos2* and *ptc* eye imaginal discs (Supplementary Figure S5).

Interestingly, in eye imaginal discs, this non-autonomous activity is position-dependent and occurs only anterior and immediately posterior to the MF. We also observed a position-dependence in the wing imaginal disc where the non-cell autonomous upregulation is restricted to the wing pouch (Figure 3d). The reason for the position-dependence is unknown, but it shows that not every tissue with deregulated Hh signaling responds to it. Some tissues appear to be inert to it. This position-dependent effect of deregulated Hh signaling has also been observed in human cancer[55] and may explain why oncogenic Hh signaling causes only certain types of cancers but not others. It is also noteworthy that even when the tissue responds to deregulated Hh signaling, the outcome can be different, too. For example, mosaic wing discs, which contain clones of activated N or are doubly mutant for *ptc* and *ark* (Apaf-1-related killer), stimulate Hippo/Warts/Yorkie signaling.[35,56] These responses appear to be a

wing-specific effect, as the eye does not respond in this way (Supplementary Figure S5).

It is estimated that deregulated Hh signaling is associated with up to 25% of human tumors.[48] Ligand-independent Hh signaling is associated with several tumors in humans such as basal cell carcinoma, medulloblastoma, rhabdomyosarcoma and glioma.[25] In most cases, genetic inactivation of *Ptch1* or activating missense mutations of *Smo* are the underlying cause of these tumors. Gene amplification of *Gli1* and *Gli2* also promotes ligand-independent Hh signaling and causes glioma and medulloblastoma.[25] Recent work in a mouse model for breast cancer that induced ligand-independent Hh signaling by expression of a constitutively active *smo* allele demonstrated a non-cell autonomous effect on proliferation that may support tumor growth.[49] Furthermore, in samples from human breast cancer patients, cells with deregulated Hh activity did not label for the proliferation marker Ki67, implying a non-cell autonomous effect of deregulated Hh signaling.[50] Although these studies focused on proliferation, we demonstrate here that deregulated Hh signaling also increases resistance to apoptosis non-cell autonomously.

The control of N by Hh signaling is conserved in mammals and occurs during normal development and in tumors, including medulloblastomas and breast cancer.[49,51,52] IAPs are upregulated in many human cancers and contribute to increased tumor cell survival.[53,54] The non-cell autonomous control of IAP levels by deregulated Hh and N signaling reveals a novel mechanism by which tumor cells and the tumor micro-environment increase cell survival.

In summary, we demonstrated that aberrant Hh signaling not only affects proliferation but also cell survival of neighboring cells. This non-cell autonomous control of apoptosis highlights an underappreciated function of Hh signaling. Potentially, the combined effects of non-cell autonomous proliferation and apoptosis resistance on the tumor micro-environment may be needed for efficient tumorigenesis.

Materials and Methods

Mutagenesis and fly stocks. The *GheF* screens are described elsewhere.[31,32] Two complementation groups were isolated in the *GheF* mutagenesis screen for 2R (right arm of chromosome 2). The first group of three alleles is mutant for *cos2*, because they fail to complement two known alleles of *cos2*, *cos2*[5] and *cos2*[k16101]. Two new alleles, *cos2*[H29] and *cos2*[P50], were chosen for sequencing. Both carry premature termination codons: *cos2*[H29] at position 15 (Arg15) and *cos2*[P50] at position 580 (Gln580). Because *cos2*[H29] has an early premature termination codon and is likely a null allele, most of the data presented in this paper were obtained for *cos2*[H29]. The second group was identified as *ptc* because they fail to complement the *ptc*[S2] allele, and point mutations were identified for two alleles. *ptc*[C] carries a premature termination codon at position 361 (Gln361) and *ptc*[L49] contains a missense mutation changing Trp775 to Arg. Mutants of *pka-C1*, located on 2L, were tested separately and also found to suppress *GMR-hid* in mosaics.

The following mutants and transgenic lines were used: *cos2*[H29], *cos2*[P50], *cos*[L51]; *ptc*[C], *ptc*[L49] (this study); *cos2*[5], *cos2*[k16101] (Bloomington); *ptc*[S2] (kind gift of Phil Ingham); *pka-C1*[K2], *pka-C1*[B3], *smo*[D16], *Su(H)*[Δ47], *UAS-CiA* (kind gift of Dan Kalderon); *UAS-CiR* ≡ *UAS-ci*[CE] (kind gift of Konrad Basler); *cul-1*[EX], *nedd8*[AN015], *slmb*[1] (kind gift of Cheng-Ting Chien); *diap1-lacZ* is *th*[5c8] (Bloomington); *N*[8], *Dl*[RevF10] *Ser*[RX82], *UAS-N*[intra] (kind gift of Hugo Bellen); *Uba1*[H42]; *tubulin-1>y*[+], *GFP>GAL4* (kind gift of Hyung Don Ryoo); *GMR-hid*; *GMR-hid ey-FLP*; *GMR-hid[w⁻]*; *E(spl)m8-2.61-lacZ* and *ex-lacZ* (*ex*[697]) (kind gift of Georg Halder); *UAS-Dl RNAi*[37287] (obtained from the Vienna DRC). Other stocks were obtained from the Bloomington stock center. *E(spl)m8-2.61-lacZ* is inserted on 2R. For analysis in *cos2* and *pka-C1* background, *E(spl)m8-2.61-lacZ* was recombined onto the *cos2*, the homologous *FRT42D P[ubi-GFP]* and the *P[ubi-GFP] FRT40* chromosomes.

Mosaic analysis. Mosaics were induced using several techniques. Generally, we used the FLP/FRT system,[57] with *ey-FLP*[58] as the enzymatic source and marking the non-mutant tissue using either *P[ubi-GFP]* to express GFP in the larval tissue or *P[w⁺]* to generate red eye pigment in adults in a *w⁻* background. The autonomy of *GMR-hid* suppression was examined with *GMR-hid[w]*, an insertion on the third chromosome.[26] *hs-FLP* was used to induce mosaic wing discs. Mosaics were also generated using the MARCM (mosaic analysis with a repressible cell marker) technique, which allows expression of transgenes such as *UAS-CiR* in mutant clones.[59]

hs-FLP was also used as the source of enzymatic activity to induce recombination using the *FLP*-out technique[60] using *FLP*-out cassettes that contain 2 FRT (>) sites flanking the marker genes; *FLP*-induced excision of the marker gene allows the promoter (*tub* or *Act5C*) to drive expression of GAL4. The following *FLP*-out cassettes were used: *hs-FLP; P[tubP>GFP>GAL4]* (Figures 3c and d) and *hs-FLP/+ ; P[Act5c>CD2>GAL4]* (Figure 4g). First instar larvae were heat-shocked for 1 h at 37 °C to induce clones.

Immunohistochemistry. Imaginal discs were dissected from third instar larvae and stained using the standard protocols. Antibodies to the following primary antigens were used: cleaved caspase 3 (CAS3*; Cell Signaling Technology, Danvers, MA, USA);[30] Diap-1 (gifts from Pascal Meier and Hyung Don Ryoo); ß-GAL (Promega, Madison, WI, USA); CD2 (Santa Cruz Biotechnology, Santa Cruz, CA, USA); Notch (clones C458.2H and C17.9C6; DSHB, Iowa City, IA, USA) and Delta (C594.9B; DSHB); Ptc (clone Apa 1; DSHB). Cy3-conjugated anti-guinea pig, anti-rat and anti-rabbit (Jackson ImmunoResearch, West Grove, PA, USA) and AlexaFluor 546-conjugated anti-mouse and anti-rabbit (Invitrogen, Grand Island, NY, USA) were used as secondary antibodies.

Imaging and analysis. Bright field imaging was performed on a Zeiss AxioImager using ApoTome technology and CZ Projection software (Zeiss, Jena, Germany). Statistical analysis was performed on bright field images using Adobe Photoshop CS4 (San Jose, CA, USA) software to quantify the size of the eye using at least 10 images per genotype; GraphPad Prism 5 (La Jolla, CA, USA) was used to generate graphs. Images of eye imaginal discs were taken using either an Olympus Fluoview 500 or Fluoview 1000 Laser Confocal Microscope (Center Valley, PA, USA) and digital images were processed using the associated software.

Conflict of Interest

The authors declare no conflict of interest.

1. Xu D, Woodfield SE, Lee TV, Fan Y, Antonio C, Bergmann A. Genetic control of programmed cell death (apoptosis) in *Drosophila*. *Fly (Austin Tex)* 2009; **3**: 78–90.
2. Fuchs Y, Steller H. Programmed cell death in animal development and disease. *Cell* 2011; **147**: 742–758.
3. Kumar S. Caspase function in programmed cell death. *Cell Death Differ* 2007; **14**: 32–43.
4. Bergmann A. The role of ubiquitylation for the control of cell death in *Drosophila*. *Cell Death Differ* 2010; **17**: 61–67.
5. Bergmann A, Steller H. Apoptosis, stem cells, and tissue regeneration. *Sci Signal* 2010; **3**: re8.
6. Fan Y, Bergmann A. Apoptosis-induced compensatory proliferation. The Cell is dead. Long live the Cell! *Trends Cell Biol* 2008; **18**: 467–473.
7. Baker NE. Patterning signals and proliferation in *Drosophila* imaginal discs. *Curr Opin Genet Dev* 2007; **17**: 287–293.

8. Roignant JY, Treisman JE. Pattern formation in the *Drosophila* eye disc. *Int J Dev Biol* 2009; **53**: 795–804.
9. Brachmann CB, Cagan RL. Patterning the fly eye: the role of apoptosis. *Trends Genet* 2003; **19**: 91–96.
10. Horsfield J, Penton A, Secombe J, Hoffman FM, Richardson H. Decapentaplegic is required for arrest in G1 phase during *Drosophila* eye development. *Development* 1998; **125**: 5069–5078.
11. Firth LC, Baker NE. Extracellular signals responsible for spatially regulated proliferation in the differentiating *Drosophila* eye. *Dev Cell* 2005; **8**: 541–551.
12. Dominguez M, Hafen E. Hedgehog directly controls initiation and propagation of retinal differentiation in the *Drosophila* eye. *Genes Dev* 1997; **11**: 3254–3264.
13. Heberlein U, Wolff T, Rubin GM. The TGF beta homolog dpp and the segment polarity gene hedgehog are required for propagation of a morphogenetic wave in the *Drosophila* retina. *Cell* 1993; **75**: 913–926.
14. Baonza A, Freeman M. Control of cell proliferation in the *Drosophila* eye by Notch signaling. *Dev Cell* 2005; **8**: 529–539.
15. Huangfu D, Anderson KV. Signaling from Smo to Ci/Gli: conservation and divergence of Hedgehog pathways from *Drosophila* to vertebrates. *Development* 2006; **133**: 3–14.
16. Jiang J, Hui CC. Hedgehog signaling in development and cancer. *Dev Cell* 2008; **15**: 801–812.
17. Ingham PW, Nystedt S, Nakano Y, Brown W, Stark D, van den Heuvel M *et al*. Patched represses the Hedgehog signalling pathway by promoting modification of the Smoothened protein. *Curr Biol* 2000; **10**: 1315–1318.
18. Denef N, Neubuser D, Perez L, Cohen SM. Hedgehog induces opposite changes in turnover and subcellular localization of Patched and Smoothened. *Cell* 2000; **102**: 521–531.
19. Robbins DJ, Nybakken KE, Kobayashi R, Sisson JC, Bishop JM, Therond PP. Hedgehog elicits signal transduction by means of a large complex containing the kinesin-related protein costal2. *Cell* 1997; **90**: 225–234.
20. Cheung HO, Zhang X, Ribeiro A, Mo R, Makino S, Puviindran V *et al*. The kinesin protein Kif7 is a critical regulator of Gli transcription factors in mammalian hedgehog signaling. *Sci Signal* 2009; **2**: ra29.
21. Endoh-Yamagami S, Evangelista M, Wilson D, Wen X, Theunissen JW, Phamluong K *et al*. The mammalian Cos2 homolog Kif7 plays an essential role in modulating Hh signal transduction during development. *Curr Biol* 2009; **19**: 1320–1326.
22. Farzan SF, Ascano M Jr., Ogden SK, Sanial M, Brigui A, Plessis A *et al*. Costal2 functions as a kinesin-like protein in the hedgehog signal transduction pathway. *Curr Biol* 2008; **18**: 1215–1220.
23. Sisson JC, Ho KS, Suyama K, Scott MP. Costal2, a novel kinesin-related protein in the Hedgehog signaling pathway. *Cell* 1997; **90**: 235–245.
24. Marks SA, Kalderon D. Regulation of mammalian Gli proteins by Costal 2 and PKA in *Drosophila* reveals Hedgehog pathway conservation. *Development* 2011; **138**: 2533–2542.
25. Teglund S, Toftgard R. Hedgehog beyond medulloblastoma and basal cell carcinoma. *Biochim Biophys Acta* 2010; **1805**: 181–208.
26. Herz HM, Chen Z, Scherr H, Lackey M, Bolduc C, Bergmann A. vps25 mosaics display non-autonomous cell survival and overgrowth, and autonomous apoptosis. *Development* 2006; **133**: 1871–1880.
27. Lee TV, Ding T, Chen Z, Rajendran V, Scherr H, Lackey M *et al*. The E1 ubiquitin-activating enzyme Uba1 in *Drosophila* controls apoptosis autonomously and tissue growth non-autonomously. *Development* 2008; **135**: 43–52.
28. Wang Y, Chen Z, Bergmann A. Regulation of EGFR and Notch signaling by distinct isoforms of D-cbl during *Drosophila* development. *Dev Biol* 2010; **342**: 1–10.
29. Wang Y, Werz C, Xu D, Chen Z, Li Y, Hafen E *et al*. *Drosophila* cbl is essential for control of cell death and cell differentiation during eye development. *PloS ONE* 2008; **3**: e1447.
30. Fan Y, Bergmann A. The cleaved-Caspase-3 antibody is a marker of Caspase-9-like DRONC activity in *Drosophila*. *Cell Death Differ* 2010; **17**: 534–539.
31. Xu D, Li Y, Arcaro M, Lackey M, Bergmann A. The CARD-carrying caspase Dronc is essential for most, but not all, developmental cell death in *Drosophila*. *Development* 2005; **132**: 2125–2134.
32. Srivastava M, Scherr H, Lackey M, Xu D, Chen Z, Lu J *et al*. ARK, the Apaf-1 related killer in *Drosophila*, requires diverse domains for its apoptotic activity. *Cell Death Differ*, 2007; 14(1): 92–102.
33. Duman-Scheel M, Weng L, Xin S, Du W. Hedgehog regulates cell growth and proliferation by inducing Cyclin D and Cyclin E. *Nature* 2002; **417**: 299–304.
34. Christiansen AE, Ding T, Bergmann A. Ligand-independent activation of the Hedgehog pathway displays non-cell autonomous proliferation during eye development in *Drosophila*. *Mech Dev* 2012; **129**: 98–108.
35. Kagey JD, Brown JA, Moberg KH. Regulation of Yorkie activity in *Drosophila* imaginal discs by the Hedgehog receptor gene patched. *Mech Dev* 2012; e-pub ahead of print 15 June 2012; doi:10.1016/j.mod.2012.05.007.
36. Ou CY, Lin YF, Chen YJ, Chien CT. Distinct protein degradation mechanisms mediated by Cul1 and Cul3 controlling Ci stability in *Drosophila* eye development. *Genes Dev* 2002; **16**: 2403–2414.
37. Hay BA, Wassarman DA, Rubin GM. *Drosophila* homologs of baculovirus inhibitor of apoptosis proteins function to block cell death. *Cell* 1995; **83**: 1253–1262.
38. Wang SL, Hawkins CJ, Yoo SJ, Muller HA, Hay BA. The *Drosophila* caspase inhibitor DIAP1 is essential for cell survival and is negatively regulated by HID. *Cell* 1999; **98**: 453–463.
39. Lisi S, Mazzon I, White K. Diverse domains of THREAD/DIAP1 are required to inhibit apoptosis induced by REAPER and HID in *Drosophila*. *Genetics* 2000; **154**: 669–678.
40. Meier P, Silke J, Leevers SJ, Evan GI. The *Drosophila* caspase DRONC is regulated by DIAP1. *EMBO J* 2000; **19**: 598–611.
41. Goyal L, McCall K, Agapite J, Hartwieg E, Steller H. Induction of apoptosis by *Drosophila* reaper, hid and grim through inhibition of IAP function. *EMBO J* 2000; **19**: 589–597.
42. Aza-Blanc P, Ramirez-Weber FA, Laget MP, Schwartz C, Kornberg TB. Proteolysis that is inhibited by hedgehog targets Cubitus interruptus protein to the nucleus and converts it to a repressor. *Cell* 1997; **89**: 1043–1053.
43. Smelkinson MG, Kalderon D. Processing of the *Drosophila* hedgehog signaling effector Ci-155 to the repressor Ci-75 is mediated by direct binding to the SCF component Slimb. *Curr Biol* 2006; **16**: 110–116.
44. Ou CY, Wang CH, Jiang J, Chien CT. Suppression of Hedgehog signaling by Cul3 ligases in proliferation control of retinal precursors. *Dev Biol* 2007; **308**: 106–119.
45. Hepker J, Wang QT, Motzny CK, Holmgren R, Orenic TV. *Drosophila* cubitus interruptus forms a negative feedback loop with patched and regulates expression of Hedgehog target genes. *Development* 1997; **124**: 549–558.
46. Halder G, Johnson RL. Hippo signaling: growth control and beyond. *Development* 2011; **138**: 9–22.
47. Bailey AM, Posakony JW. Suppressor of hairless directly activates transcription of enhancer of split complex genes in response to Notch receptor activity. *Genes Dev* 1995; **9**: 2609–2622.
48. Briscoe J, Therond P. Hedgehog signaling: from the *Drosophila* cuticle to anti-cancer drugs. *Dev Cell* 2005; **8**: 143–151.
49. Visbal AP, LaMarca HL, Villanueva H, Toneff MJ, Li Y, Rosen JM *et al*. Altered differentiation and paracrine stimulation of mammary epithelial cell proliferation by conditionally activated Smoothened. *Dev Biol* 2011; **352**: 116–127.
50. Moraes RC, Zhang X, Harrington N, Fung JY, Wu MF, Hilsenbeck SG *et al*. Constitutive activation of Smoothened (SMO) in mammary glands of transgenic mice leads to increased proliferation, altered differentiation and ductal dysplasia. *Development* 2007; **134**: 1231–1242.
51. Hallahan AR, Pritchard JI, Hansen S, Benson M, Stoeck J, Hatton BA *et al*. The SmoA1 mouse model reveals that notch signaling is critical for the growth and survival of sonic hedgehog-induced medulloblastomas. *Cancer Res* 2004; **64**: 7794–7800.
52. Sengupta A, Banerjee D, Chandra S, Banerji SK, Ghosh R, Roy R *et al*. Deregulation and cross talk among Sonic hedgehog, Wnt, Hox and Notch signaling in chronic myeloid leukemia progression. *Leukemia* 2007; **21**: 949–955.
53. LaCasse EC, Mahoney DJ, Cheung HH, Plenchette S, Baird S, Korneluk RG. IAP-targeted therapies for cancer. *Oncogene* 2008; **27**: 6252–6275.
54. Gyrd-Hansen M, Meier P. IAPs: from caspase inhibitors to modulators of NF-kappaB, inflammation and cancer. *Nat Rev Cancer* 2010; **10**: 561–574.
55. Stecca B, Ruiz IAA. Context-dependent regulation of the GLI code in cancer by HEDGEHOG and non-HEDGEHOG signals. *J Mol Cell Biol* 2010; **2**: 84–95.
56. Graves HK, Woodfield SE, Yang CC, Halder G, Bergmann A. Notch signaling activates Yorkie non-cell autonomously in *Drosophila*. *PloS One* 2012; **7**: e37615.
57. Xu T, Rubin GM. Analysis of genetic mosaics in developing and adult *Drosophila* tissues. *Development* 1993; **117**: 1223–1237.
58. Newsome TP, Asling B, Dickson BJ. Analysis of *Drosophila* photoreceptor axon guidance in eye-specific mosaics. *Development* 2000; **127**: 851–860.
59. Lee T, Luo L. Mosaic analysis with a repressible cell marker (MARCM) for *Drosophila* neural development. *Trends Neurosci* 2001; **24**: 251–254.
60. Struhl G, Basler K. Organizing activity of wingless protein in *Drosophila*. *Cell* 1993; **72**: 527–540.